tvst

Article

Quantitative Evaluation of Retinal Microvascular Abnormalities in Patients With Type 2 Diabetes Mellitus Without Clinical Sign of Diabetic Retinopathy

Yongqing Han[1,*], Xiaogang Wang[2,*], Gang Sun[3], Jing Luo[4], Xing Cao[4], Pengyi Yin[4], Renhe Yu[5], Simin He[5], Fang Yang[5], Frank L. Myers[6], and Liang Zhou[4]

[1] Department of Ophthalmology, Affiliated Hospital of Inner Mongolia Minzu University, Tongliao, Inner Mongolia, P.R. China
[2] Department of Ophthalmology, Shanxi Eye Hospital, Taiyuan, Shanxi, P.R. China
[3] Department of Intelligence and Collaboration, Yangzhou Collaborative Innovation Research Institute of Shenyang Aircraft Design and Research Institute, Yangzhou, Jiangsu, P.R. China
[4] Department of Ophthalmology, the Second Xiangya Hospital, Central South University, Changsha, Hunan, P.R. China
[5] Department of Epidemiology and Health Statistics, Xiangya School of Public Health, Central South University, Changsha, Hunan, P.R. China
[6] Department of Ophthalmology and Visual Sciences, University of Wisconsin-Madison School of Medicine and Public Health, Madison, WI, USA

Correspondence: Liang Zhou, Department of Ophthalmology, The Second Xiangya Hospital, Central South University, 139 Middle Renmin Road, Hunan 410011, P.R. China.
e-mail: zhouliang12@csu.edu.cn

Received: September 2, 2021
Accepted: March 26, 2022
Published: April 21, 2022

Keywords: diabetic retinopathy; optical coherence tomography angiography; FD-300

Citation: Han Y, Wang X, Sun G, Luo J, Cao X, Yin P, Yu R, He S, Yang F, Myers FL, Zhou L. Quantitative evaluation of retinal microvascular abnormalities in patients with type 2 diabetes mellitus without clinical sign of diabetic retinopathy. Transl Vis Sci Technol. 2022;11(4):20, https://doi.org/10.1167/tvst.11.4.20

Purpose: To evaluate microvascular abnormalities in the macula and peripapillary area in diabetic patients without clinical signs of diabetic retinopathy (DR) and compare them with healthy control eyes, using optical coherence tomography angiography (OCTA).

Methods: A prospective study was performed of 49 eyes from 49 diabetic patients without clinical signs of DR and a control group of 52 eyes from 52 healthy normal individuals. The 3 × 3 mm macular scans and 4.5 × 4.5 mm optic disc scans were obtained with the OCTA RTVue-XR Avanti system. Angiograms from the superficial capillary plexus, the deep capillary plexus of the macula scans, and radial peripapillary capillary plexus of the optic disc scans were analyzed with MATLAB. Multivariate binary logistic regression and the least absolute shrinkage and selection operator (LASSO) regression were used to select ideal parameters that distinguish diabetic eyes without DR from normal eyes. A receiver operating characteristic (ROC) curve was generated, and sensitivity and specificity were calculated.

Results: Our final model identified FD-300 (foveal vessel density in a 300-µm-wide region around foveal avascular zone) as the only parameter selected by both the LASSO regression and the final multivariate logistic regression model that significantly differentiates diabetic eyes without clinical signs of DR from healthy normal eyes. The area under the ROC curve of FD-300 was 0.685, and sensitivity and specificity were 65.3% and 71.2%, respectively.

Conclusions: Quantitative evaluation of retinal microvascular abnormalities using OCTA identified FD-300 as a useful biomarker versus the other macular and peripapillary OCTA metrics in the early detection of preclinical diabetic retinal abnormalities.

Translational Relevance: OCTA may be useful in detecting early retinal microvascular abnormalities in diabetic patients before the clinical findings of DR become visible.

Introduction

Diabetes mellitus is one of the most common vascular diseases worldwide, affecting 400 million globally and more than 20 million in China.[1] As the leading cause of blindness in working-age adults, the prevalence of diabetic retinopathy (DR) was 6.6% in diabetic patients afflicted with diabetes mellitus for less than 5 years, whereas the number increased to more than

52.7% in those with the disease for more than 20 years.[2] The retinal microvasculature is the main target of high blood glucose, leading to microaneurysms, hard exudates, retinal ischemia, and hemorrhages, which are the clinical findings related to the diagnosis of diabetic retinopathy.[3] Preclinical findings of DR are important for early diagnosis and intervention, which may help these patients avoid deterioration of the retinal condition.

As a novel, noninvasive imaging technology, optical coherence tomography angiography (OCTA) can demonstrate the retinal microvasculature without the administration of exogenous dyes. Using commercial OCTA devices, three retinal vascular networks are automatically segmented: the superficial capillary plexus (SCP), the deep capillary plexus (DCP), and the radial peripapillary capillary plexus (RPCP), which runs parallel with the retinal nerve fiber layer (RNFL).[4] Several studies have reported abnormal vasculature parameters including macular vessel density in the SCP or the DCP, peripapillary RPCP density, and RNFL thickness in diabetic eyes without clinical signs of DR compared with normal controls.[5–8] However, there is a lack of a comprehensive view of the density and the morphology of the retinal microvasculature in the early stages of diabetic eyes, including both the parafoveal and the peripapillary areas.

In this study, we quantified the retinal microvasculature from both macular and optic disc OCTA scans using an automated MATLAB program (MathWorks, Inc., Natick, MA, USA). The foveal avascular zone (FAZ) metrics include FAZ area, FAZ perimeter, acircularity index (AI), and FD-300 (foveal vessel density in a 300-µm-wide region around FAZ). Vessel density indexes include vessel density and extrafoveal avascular area (EAA). Vessel morphology indexes include vessel length fraction (VLF), fractal dimension and vessel diameter index (VDI). The current study compares the macular and peripapillary OCTA metrics in diabetic patients without clinical signs of DR with those of healthy individuals to determine the strongest biomarkers that can be used to differentiate the two groups.

Methods

Design

This is a prospective cross-sectional study comparing OCTA data from diabetic patients without clinical signs of DR and normal controls of comparable age. The study protocol analyzed several modes of the OCTA scans to produce metrics that were then compared between the two groups. The angiography images were collected from the Affiliated Hospital of Inner Mongolia University for the Nationalities. The study protocol was approved by the Medical Ethics Committee of Affiliated Hospital of Inner Mongolia University for the Nationalities following the principles of the Declaration of Helsinki. Written informed consent was obtained from all study participants.

Participants

Between 2018 and 2021, 49 patients with type 2 diabetes mellitus without clinical signs of DR and 52 healthy individuals from the clinics of the Ophthalmology department in Affiliated Hospital of Inner Mongolia University for the Nationalities were recruited. Exclusion criteria included (1) eyes with any visible retinal pathology findings such as microaneurysm, hemorrhages, hard exudates or cotton-wool spots seen on clinical examination and color fundus photography; (2) patients with astigmatism, or moderate to high refractive error (more than 3 diopters); (3) scan quality score below 7 (10 as full score), inaccurate segmentation of retinal layer or slabs, significant image artifacts, shadow or blur of the image, or poor centration; (4) history of panretinal photocoagulation, intravitreal injection or any ocular surgeries; and (5) intraocular pressure higher than 21 mm Hg or glaucoma suspects.

All participants included in the study were checked by two experienced retinal specialists. Best-corrected visual acuity (BCVA), intraocular pressure, slit-lamp and fundus examination were performed. Refraction was performed first with an auto refractometer (Topcon KR-800; Topcon Optical Company, Tokyo, Japan) and then checked by trained personnel for the final refraction. BCVA was determined for all subjects using Tumbling E charts and converted to the logMAR as described previously.

OCTA Imaging

All of the participants underwent OCTA scanning using the RTVue-XR Avanti system (Optovue, Inc., Fremont, CA, USA), which used a speed of 70,000 A-scans per second. We obtained 3 × 3 mm scans centered on the fovea and 4.5 × 4.5 mm scans centered on the optic disc.

The SCP and the DCP of the macula and the RPCP of the peripapillary retina were all segmented automatically by the built-in software (RTVue XR, Version 2018.1.0.43). The SCP was defined as a retinal layer between the inner limiting membrane and 10 µm above the inner plexiform layer. The DCP was defined as

a retinal layer between 10 µm above the inner plexiform layer and 10 µm below the outer plexiform layer. The RPCP was defined as the layer between the inner limiting membrane and the posterior boundary of the retinal nerve fiber layer. To avoid projections of large vessels from the superficial layer of the retina, and to make the analysis of the DCP more accurate and reliable, the new algorithm of projection artifact removal was used in the updated Optovue equipment.[9]

Quantification of Retinal Microvasculature

All OCTA images were analyzed with the MATLAB program. FAZ metrics, including the FAZ area, FAZ perimeter, acircularity index and FD-300, were evaluated in a combined SCP and DCP angiographic image. Vessel density and morphology metrics, including VD, EAA, VLF, fractal dimension and VDI, were assessed for both SCP and DCP on 3 × 3 mm macular scans. VD, VLF, fractal dimension and VDI were assessed for RPCP on 4.5 × 4.5 mm optic disc scans. Vessel density (VD) for the 3 × 3 mm macular scans were assessed in an annulus area with an inner and outer ring diameter of 1 mm and 3 mm, both centered on the fovea. VD for the 4.5 × 4.5 mm optic disc scan was assessed in an annulus area with an inner and outer ring diameter of 2 mm and 4 mm, both centered on the center of the disc. VD in both the whole annulus area and four different quadrants (inferior, nasal, superior, temporal) were analyzed.

Acircularity index was defined as the ratio of the perimeter of the FAZ to the perimeter of a circle equal area, as

$$AI = \frac{\text{FAZ\_perimeter}}{2\pi\sqrt{s/\pi}}$$

where AI is the acircularity index, FAZ_perimeter is the perimeter of the FAZ, and S indicates the area of FAZ.

FD-300 is defined as the foveal vessel density of the 300 µm width ring surrounding the FAZ. To obtain FD-300, the 300 µm width ring must first be accurately located; then, vessel density within the ring will be calculated. The main steps are (1) localize FAZ boundary as the inner boundary of the 300 µm width ring by an active contour method described in the reference.[10] In this step, the initial region of this active contour is a 20 × 20 box in the image center; (2) localize the outer boundary of the 300 µm width ring by extending the inner boundary 300 µm outward; (3) the 300 µm width ring is now located by the inner and outer boundaries. Vessel density within this ring is obtained by dividing the number of vessels pixels by the total number of pixels.

VD is calculated as the percentage of vessels within statistical zones. To do this, vessels are first segmented by the Otsu thresholding method.[11] The VD is obtained as follows:

$$VD = \frac{\left(\sum_{(i,j)}^{n} V_{(i,j)}\right)}{\left(\sum_{(i,j)}^{n} I_{(i,j)}\right)}$$

where $V_{(i,j)}$represents vascular pixels within statistical zones and $I_{(i,j)}$represents pixels within statistical zones (including vessel and non-vessel pixels).

Extrafoveal avascular area (EAA) is calculated as the percentage of avascular area outside a 1-mm circle with the same center point of the image, as previously described.[12] First, a binary vessel image is obtained by the Local Otsu thresholding method, described in the reference.[13] Then, Euclidean distance transform is applied to the binary vessel image, producing the vessel distance map. Next, erosion operations are applied to the vessel distance map with a five-pixel-wide square kernel. Finally, areas smaller than eight pixels in the vessel distance map are eliminated, and dilation operations are applied by a seven-pixel-wide square kernel.

VLF measures retinal vessel length. VDI measures the averaged vessel caliber. To analyze these two parameters, skeletonized images were obtained by extracting the centerline of blood vessels, VLF is then calculated by dividing vessel centerline pixels by total pixels as follows:

$$VLF = \frac{\left(\sum_{(i,j)}^{n} C_{(i,j)}\right)}{\left(\sum_{(i,j)}^{n} I_{(i,j)}\right)}$$

where $C_{(i,j)}$represents vascular centerline pixels within statistical zones and $I_{(i,j)}$represents pixels within statistical zones (including pixels of vessel centerlines and non-vessel centerlines).

VDI is calculated by dividing total vascular pixels by vessel centerline pixels. To do this, vessels are first segmented by Otsu's thresholding method,[11] then vascular centerlines are extracted from vessels by thinning methodologies.[14] Next, the VDI is obtained as follows:

$$VDI = \frac{\left(\sum_{(i,j)}^{n} V_{(i,j)}\right)}{\left(\sum_{(i,j)}^{n} C_{(i,j)}\right)}$$

where $V_{(i,j)}$represents vascular pixels within statistical zones and $C_{(i,j)}$represents vascular centerline pixels within statistical zones.

Fractal dimension reflects the geometry and complexity of retinal vessel branching architecture.

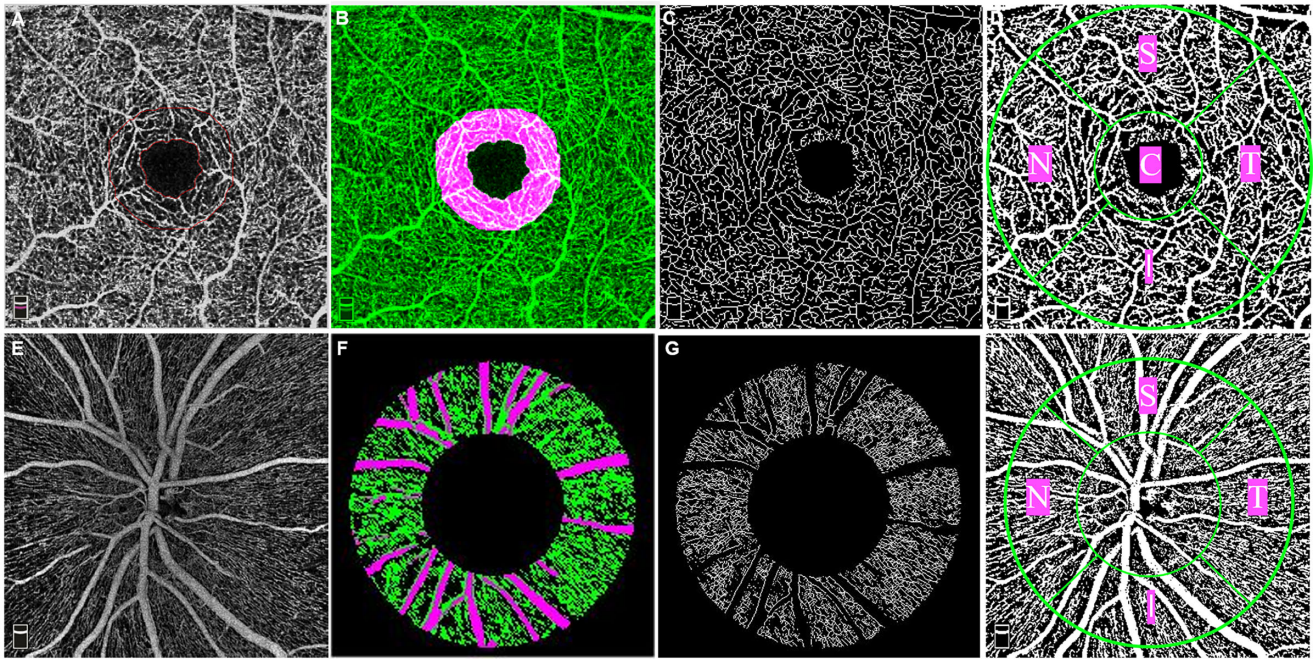

Figure 1. Image processing procedure for the 3 × 3 mm macular scan (**A–D**) and 4.5 × 4.5 mm optic disc scan (**E–H**) in a left eye. (**A**) FAZ (inner circle) and the ring area where FD-300 is measured (the region between the inner and outer circle which is 300-µm-wide) in a combined SCP and DCP image. (**B**) The region where FD-300 is measured is marked as *pink*, and the vessel network is marked as *green*. (**C**) Skeletonized image of the parafoveal microvasculature in the superficial capillary plexus. (**D**) Binary vessel image for the vessel density analysis showing five different sectors (C = central, S = superior, N = nasal, I = inferior, T = temporal). (**E**) OCTA image of the RPCP in the peripapillary area. (**F**) Annulus area with an inner and outer ring diameter of 2 mm and 4 mm both centered on the center of the disc. The vessel network is marked as *green*, large vessels are marked as *pink*. (**G**) Skeletonized image of peripapillary microvasculature with large vessels being masked. (H) Binary vessel image for the vessel density analysis showing four different sectors (S = superior, N = nasal, I = inferior, T = temporal).

The fractal dimension was calculated over the skeletonized image using a box-counting technique, which was reported in the literature.[15]

It is noted that, for optic disc images, large vessels are removed by the method described in the reference.[13] Only the small vessels within 2 mm width ring surrounding the image center will be calculated. In contrast, for 3 × 3 mm macular images, no large vessels are excluded from the calculation. The methods are modified from previous publications.[13,16]

Figure 1 demonstrates examples of the OCTA processing procedure in the left eye of one 52-year-old male diabetic patient who had been diagnosed with diabetes mellitus for 3 years but without clinical findings of DR.

Statistical Analysis

Statistical analysis was performed using SPSS (SPSS for Windows, version 24.0, IBM Corp) and R software (version 4.0.4). An independent *t*-test was used to compare variables that followed a normal distribution. The variables following a skewed distribution were compared using a Mann-Whitney test. Selected parameters were then introduced as dependent variables in a multivariate binary logistic regression model. The least absolute shrinkage and selection operator (LASSO) regression was also applied to all the variates to select significant parameters that distinguish the two groups. LASSO is a penalized regression approach that penalizes the absolute value of a regression coefficient.[17] The greater the penalization, the greater the shrinkage of coefficients; with some coefficients reaching 0, LASSO automatically deletes unnecessary covariates.[17] The receiver operating characteristic (ROC) curves were generated for the parameters that were significant in the final statistical model. The area under the curve (AUC), sensitivity and specificity were then calculated.

Results

A total of 101 eyes were included in this study, including 49 eyes of diabetic patients without clinical

Table 1. Demographic Characteristics of Diabetic Patients Without Clinical Signs of Diabetic Retinopathy and Healthy Control Individuals

	Normal Controls (52 Eyes, Mean ± SD)	Diabetic Eyes Without Clinical Signs of DR(49 Eyes, Mean ± SD)	*P*
Age (y)	50.37 ± 10.98	51.59 ± 10.99	0.627
Sex			0.337
Male	28	31	
Female	24	18	
Duration of DM (y)		5.82 ± 4.58	
BCVA, LogMAR (Snellen equivalent)	0.0346 (20/20) ± 0.0520	0.0367(20/20) ± 0.0528	0.833
3 mm-scan quality	8.46 ± 0.67	8.55 ± 0.91	0.368
4.5-scan quality	8.67 ± 0.71	8.55 ± 0.87	0.588
Central retinal thickness (µm)	245.75 ± 16.92	246.24 ± 19.72	0.892

SD, deviation; DM, diabetes mellitus.
A value of $P < 0.05$ was considered statistically significant.

retinopathy (49 patients, 31 male and 18 female) and 52 eyes of healthy age-matched individuals (52 subjects, 28 male and 24 female). The demographic characteristics of the participants are reported in Table 1. There was no statistical difference between the two groups in the characteristics including age, sex, BCVA, intraocular pressure, 3 × 3 mm macular scan quality, 4.5 × 4.5 mm optic disc scan quality, or central retinal thickness (all $P > 0.05$).

Table 2 shows the comparison of parameters between the two groups in the parafoveal SCP, DCP, and peripapillary RPCP using univariate analysis. In the analysis, parameters in the SCP and DCP alone did not show a significant difference between these two groups. FD-300, which measures the vessel density within a 300 µm wide region of the FAZ in a combined network of both SCP and DCP, was significantly decreased in the diabetic eyes without clinical signs of DR when compared to normal controls (48.90% ± 3.45% vs. 51.18% ± 3.16%, $P = 0.001$). In the peripapillary RPCP, vessel density in the inferior quadrant and the fractal dimension of capillaries were significantly different between these two groups (46.78% ± 8.39% vs. 50.09% ± 8.16%, $P = 0.047$ and 1.67% ± 2.72% vs. 1.68% ± 2.03%, $P = 0.024$, respectively).

The three parameters were introduced as dependent variables in a multivariate binary regression model. FD-300 was still the only parameter that showed significance in the final multivariate model after adjusting for age and sex (odds ratio 3.582, 95% confidence interval 1.455–8.817, $P = 0.006$, Table 3). LASSO regression analysis also found FD-300 to be the only significant parameter that distinguished the diabetic eyes without DR from the normal controls (Fig. 2A). ROC curves were generated for the FD-300 and the AUC, and the sensitivity and specificity were calculated (0.685, 65.3%, and 71.2% respectively, Fig. 2B).

Discussion

This study compares demographic parameters and OCTA metrics in both the parafoveal area (SCP and DCP) and the peripapillary area (RPCP) between diabetic patients without clinical signs of retinopathy and healthy normal controls and provides a comprehensive view of the capillary network abnormalities in diabetic eyes without clinical signs of DR. The FD-300 was significant in LASSO regression, as well as in the final multivariate binary logistic model. The AUC of the FD-300 was 0.685, with a sensitivity and specificity of 65.3% and 71.2%, respectively. This indicates that the FD-300 is a useful biomarker that may be superior to other macular and peripapillary parameters in the early detection of DR before clinical findings become apparent.

In the center of the macula, the retinal capillary plexus merges and forms a ring that surrounds a vascular-free area called the FAZ.[18] In 2015, de Carlo et al.[19] realized that the FAZ remodeling and capillary nonperfusion were early OCTA findings in diabetic patients who did not have retinopathy. An enlargement of the FAZ was detected in the SCP and the DCP in both diabetic children and adults without clinical findings of DR.[7,20] Vujosevic et al.[7] found that the FAZ area was significantly larger in the DCP in type 2 diabetes mellitus patients without DR when compared to healthy controls. In our study, none of the FAZ area,

Table 2. Comparison of OCTA Metrics Between Diabetic Eyes Without Clinical Signs of Diabetic Retinopathy and Healthy Controls Using Univariate Analysis

	Normal Controls (52 Eyes, Mean ± SD)	Diabetic Eyes Without Clinical Signs of DR (49 Eyes, Mean ± SD)	*P* Value
FAZ associated parameters (3 mm × 3 mm)			
FAZ area, mm^2	0.35 ± 0.10	0.32 ± 0.11	0.211
FAZ perimeter, mm	2.38 ± 0.39	2.28 ± 0.40	0.197
AI	1.15 ± 0.06	1.14 ± 0.04	0.932
FD-300	51.18% ± 3.16%	48.90% ± 3.45%	0.001*
Superficial retinal layer (3 mm × 3 mm)			
VD_all	45.70% ± 4.96%	44.37% ± 4.24%	0.602
VD_central	29.30% ± 4.46%	28.89% ± 5.04%	0.160
VD_temporal	46.88% ± 5.07%	45.80% ± 4.49%	0.676
VD_superior	48.14% ± 5.26%	46.54% ± 0.04%	0.091
VD_inferior	47.42% ± 6.05%	46.13% ± 0.04%	0.267
VD_nasal	47.32% ± 4.78%	45.87% ± 0.04%	0.616
EAA, mm^2	0.0009 ± 0.0016	0.0032 ± 0.0093	0.148
VLF	0.07 ± 0.01	0.07 ± 0.01	0.676
Fractal dimension	1.75 ± 0.01	1.75 ± 0.02	0.716
VDI	7.01 ± 0.241	7.08 ± 0.29	0.229
Deep retinal layer (3 mm × 3 mm)			
VD_all	47.88% ± 4.17%	47.41% ± 4.76%	0.796
VD_central	20.36% ± 4.72%	21.80% ± 5.48%	0.160
VD_temporal	50.00% ± 4.25%	49.61% ± 5.04%	0.817
VD_superior	51.45% ± 4.87%	50.85% ± 5.89%	0.760
VD_inferior	51.55% ± 5.19%	50.37% ± 5.46%	0.236
VD_nasal	49.67% ± 4.72%	49.17% ± 5.34%	0.957
EAA, mm^2	0.0003 ± 0.0014	0.0005 ± 0.0017	0.411
VLF	0.08 ± 0.01	0.08 ± 0.01	0.128
Fractal dimension	1.75 ± 0.01	1.75 ± 0.01	0.114
VDI	5.49 ± 0.10	5.51 ± 0.12	0.932
Peripapillary RPCP (4.5 mm × 4.5 mm)			
VD-whole area	50.43% ± 7.34%	47.64% ± 7.99%	0.070
VD-temporal	55.20% ± 6.75%	52.15% ± 8.07%	0.065
VD-superior	49.12% ± 8.31%	46.73% ± 8.81%	0.164
VD-inferior	50.09% ± 8.16%	46.78% ± 8.39%	0.047*
VD-nasal	46.71% ± 8.30%	44.29% ± 8.64%	0.153
VLF	0.07 ± 0.01	0.07 ± 0.01	0.052
Fractal dimension	1.68 ± 0.02	1.67 ± 0.03	0.024*
VDI	8.05 ± 0.41	8.21 ± 0.48	0.053

SD, standard deviation; AI, acircularity index; VD, vessel density.
*$P < 0.05$ was considered a statistically significant difference between the groups.

FAZ perimeter or acircularity index show any difference between groups, which is in accordance with previous studies.[6,21] In addition, the FAZ area and the FAZ perimeter had a great variation among normal healthy individuals.[22] As a result, FD-300 as a metric reflecting the capillary loss in the parafoveal area was recently introduced in OCTA studies. Ragkousis et al.[23] and Li et al.[24] had reported that the FD-300 has a strong inverse correlation with DR severity. In the studies by Li et al.[25] and Liu et al.,[26] no difference in the FD-300 was found between diabetic eyes without DR and healthy control subjects. However, Yang et al.[27]

Table 3. Binary Logistic Regression Model for The Parameters That Selected by the Univariate Analysis

Variates	b	S_b	Wald χ^2	*P* Value	Odds Ratio	95% Confidence Interval
No adjusting for age and sex, 101 eyes of 101 patients						
FD-300	1.221	0.438	7.756	0.005*	3.391	1.436–8.007
RPCP-VD-inferior	0.159	0.595	0.071	0.790	1.172	0.365–3.764
RPCP-fractal dimension	0.588	0.613	0.920	0.337	1.800	0.541–5.987
Adjusting for age and sex, 101 eyes of 101 patients						
FD-300	1.276	0.460	7.704	0.006*	3.582	1.455–8.817
RPCP-VD-inferior	0.126	0.601	0.044	0.834	1.134	0.349–3.685
RPCP-fractal dimension	0.614	0.619	0.984	0.321	1.847	0.549–6.212

VD, vessel density.
*$P < 0.05$ was considered a statistically significant difference between the groups.

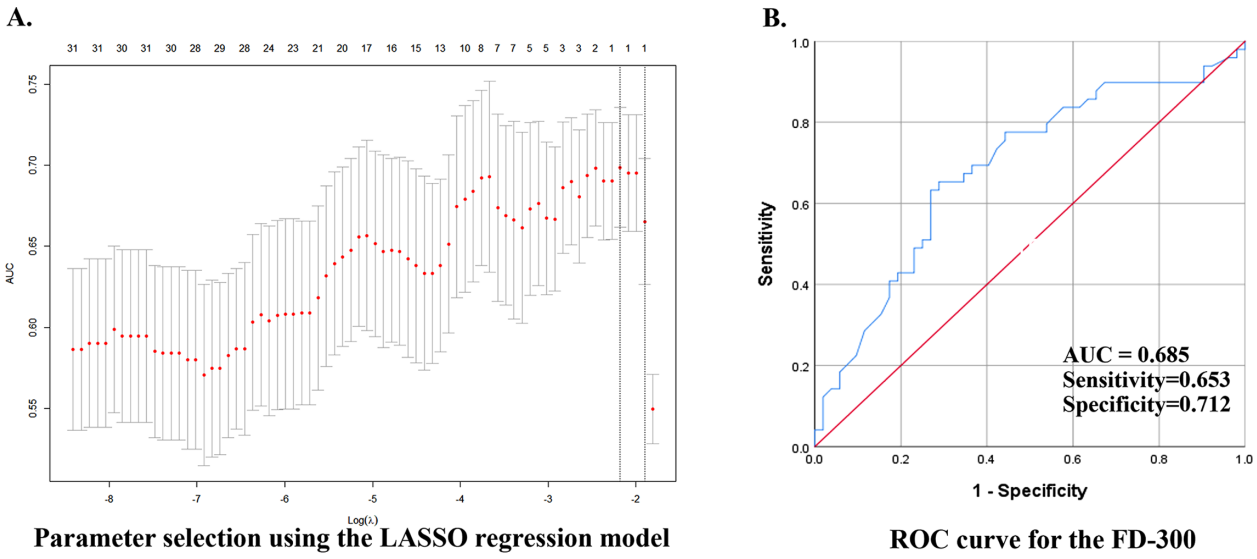

Figure 2. LASSO was used to screen the parameters, and ROC curve was used to evaluate the diagnostic ability of the selected parameter. (**A**) LASSO regression model selected FD-300 from the 32 candidate variables. (**B**) ROC curve for the FD-300.

found it significantly decreased in preclinical DR in diabetes type 2 patients. Also, Inanc et al.[28] found it to be an early biomarker in type 1 diabetic children without clinically detectable DR. After comparison with a binary logistic regression model, as well as the LASSO regression screening program, we found the FD-300 to be the strongest parameter that differentiates the preclinical diabetic group from the control group.

Peripapillary RPCP is a layer containing long radial capillaries that travel alongside the nerve fibers, and the vessel density is correlated with the retinal nerve fiber layer thickness. The loss of capillary network in the RPCP had been reported in preclinical diabetic patients before the drop out of capillaries in the macular area.[7,22,29] Fractal analysis of the peripapillary vessels has been introduced in detecting early retinal abnormalities in DR, using fundus color images and OCTA. In a study based on the color fundus photographs, lower fractal dimension is correlated with the presence of diabetic neuropathy even with no or early DR.[30] In our study, which was based on the OCTA images, the fractal dimension in the peripapillary RPCP was not as significant when compared with the FD-300 in the final statistic models. This indicates that the decreased vessel density in the foveal area may be more useful than the microvascular abnormalities in the peripapillary RPCP in differentiating diabetic patients without visible DR from normal controls.

Other vessel density and morphology abnormalities have been reported in diabetic patients without DR when compared to normal eyes, such as vessel density and fractal dimension in the DCP and the EAA of the SCP.[6,26,29] In our previous studies, the EAA of

the SCP was found to be the most sensitive biomarker in distinguishing diabetic eyes without clinical signs of DR from nonproliferative DR with high sensitivity and specificity.[31] However, in this study, none of these parameters showed significance in differentiation between the diabetic eyes without clinical findings of DR and normal controls.

In this study, we found LASSO as a powerful statistical method for determining the ideal parameter that can distinguish with high efficiency the two groups from a number of variates.

The limitations in this study include modest sample size and small scan areas (3 × 3 mm for the macula and 4.5 × 4.5 mm for the optic disc). A larger sample size is needed in further studies. Furthermore, the fractal dimensions of the RPCP are not available in the commercial OCTA equipment and, hence, cannot be observed in the clinic at present. Additionally, although FD-300 is the most efficient parameter that we have found in this study, the AUC value, sensitivity, and specificity of this parameter are generally considered acceptable.

In conclusion, we found that the FD-300 may be the strongest biomarker among the macular and peripapillary OCTA parameters in detecting preclinical diabetic abnormalities in the retina. OCTA may serve as a noninvasive technique for understanding the early pathophysiology of DR.

Acknowledgments

Supported by the National Natural Science Foundation of China (grant no. 81971697, 81501544, 81200697), the Scientific Research Project of Hunan Provincial Health Commission (grant no. 202107020970), and the Natural Science Foundation of Hunan Province (grant no. 2021JJ30982).

Disclosure: **Y. Han,** None; **X. Wang,** None; **G. Sun,** None; **J. Luo,** None; **X. Cao,** None; **P. Yin,** None; **R. Yu,** None; **S. He,** None; **F. Yang,** None; **F.L. Myers,** None; **L. Zhou,** None

* YH and XW contributed equally to this work.

References

1. Wang FH, Liang YB, Zhang F, et al. Prevalence of diabetic retinopathy in rural China: the Handan Eye Study. *Ophthalmology*. 2009;116:461–467.
2. Voigt M, Schmidt S, Lehmann T, et al. Prevalence and progression rate of diabetic retinopathy in type 2 diabetes patients in correlation with the duration of diabetes. *Exp Clin Endocrinol Diabetes*. 2018;126:570–576.
3. Emanuelsson F, Marott S, Tybjaerg-Hansen A, Nordestgaard BG, Benn M. Impact of glucose level on micro- and macrovascular disease in the general population: a mendelian randomization study. *Diabetes Care*. 2020;43:894–902.
4. Campbell JP, Zhang M, Hwang TS, et al. Detailed vascular anatomy of the human retina by projection-resolved optical coherence tomography angiography. *Sci Rep*. 2017;7:42201.
5. Rosen RB, Andrade Romo JS, Krawitz BD, et al. Earliest evidence of preclinical diabetic retinopathy revealed using optical coherence tomography angiography perfused capillary density. *Am J Ophthalmol*. 2019;203:103–115.
6. Simonett JM, Scarinci F, Picconi F, et al. Early microvascular retinal changes in optical coherence tomography angiography in patients with type 1 diabetes mellitus. *Acta Ophthalmol*. 2017;95:e751–e755.
7. Vujosevic S, Muraca A, Alkabes M, et al. Early microvascular and neural changes in patients with type 1 and type 2 diabetes mellitus without clinical signs of diabetic retinopathy. *Retina*. 2019;39:435–445.
8. Yasin Alibhai A, Moult EM, Shahzad R, et al. Quantifying microvascular changes using OCT angiography in diabetic eyes without clinical evidence of retinopathy. *Ophthalmol Retina*. 2018;2:418–427.
9. Binotti WW, Romano AC. Projection-resolved optical coherence tomography angiography parameters to determine severity in diabetic retinopathy. *Invest Ophthalmol Vis Sci*. 2019;60:1321–1327.
10. Li C, Xu C, Gui C, Fox MD. Distance regularized level set evolution and its application to image segmentation. *IEEE Trans Image Process*. 2010;19:3243–3254.
11. Shoelson B. Performs LOCAL Otsu thresholding on an image; user can specify blocksize. *Local Otsu Threshold Im2bw Uneven Background Illumination Image*.
12. Zhang M, Hwang TS, Dongye C, Wilson DJ, Huang D, Jia Y. Automated quantification of nonperfusion in three retinal plexuses using projection-resolved optical coherence tomography angiography in diabetic retinopathy. *Invest Ophthalmol Vis Sci*. 2016;57:5101–5106.

13. Pappelis K, Jansonius NM. Quantification and repeatability of vessel density and flux as assessed by optical coherence tomography angiography. *Transl Vis Sci Technol*. 2019;8:3.
14. Lam L, Lee S-W, Suen CY. Thinning methodologies-a comprehensive survey. *Pattern Analysis and Machine Intelligence, IEEE Transactions on*. 1992;14:869–885.
15. Reishofer G, Koschutnig K, Enzinger C, Ebner F, Ahammer H. Fractal dimension and vessel complexity in patients with cerebral arteriovenous malformations. *PLoS One*. 2012;7:e41148.
16. Frizziero L, Parrozzani R, Londei D, Pilotto E, Midena E. Quantification of vascular and neuronal changes in the peripapillary retinal area secondary to diabetic retinopathy. *Br J Ophthalmol*. 2021;105:1577–1583.
17. Ranstam J, Cook JA. LASSO regression. *J Br Surg*. 2018;105:1348.
18. Hormel TT, Jia Y, Jian Y, et al. Plexus-specific retinal vascular anatomy and pathologies as seen by projection-resolved optical coherence tomographic angiography. *Prog Retin Eye Res*. 2021;80:100878.
19. de Carlo TE, Chin AT, Bonini Filho MA, et al. Detection of microvascular changes in eyes of patients with diabetes but not clinical diabetic retinopathy using optical coherence tomography angiography. *Retina*. 2015;35:2364–2370.
20. Niestrata-Ortiz M, Fichna P, Stankiewicz W, Stopa M. Enlargement of the foveal avascular zone detected by optical coherence tomography angiography in diabetic children without diabetic retinopathy. *Graefes Arch Clin Exp Ophthalmol*. 2019;257:689–697.
21. Krawitz BD, Mo S, Geyman LS, et al. Acircularity index and axis ratio of the foveal avascular zone in diabetic eyes and healthy controls measured by optical coherence tomography angiography. *Vision Res*. 2017;139:177–186.
22. Linderman RE, Muthiah MN, Omoba SB, et al. Variability of foveal avascular zone metrics derived from optical coherence tomography angiography images. *Transl Vis Sci Technol*. 2018;7:20.
23. Ragkousis A, Kozobolis V, Kabanarou S, et al. Vessel density around foveal avascular zone as a potential imaging biomarker for detecting preclinical diabetic retinopathy: an optical coherence tomography angiography study. *Semin Ophthalmol*. 2020;35:316–323.
24. Li X, Xie J, Zhang L, et al. Identifying microvascular and neural parameters related to the severity of diabetic retinopathy using optical coherence tomography angiography. *Invest Ophthalmol Vis Sci*. 2020;61:39.
25. Li Z, Alzogool M, Xiao J, Zhang S, Zeng P, Lan Y. Optical coherence tomography angiography findings of neurovascular changes in type 2 diabetes mellitus patients without clinical diabetic retinopathy. *Acta Diabetologica*. 2018;55:1075–1082.
26. Liu L, Jian G, Bao W, et al. Analysis of foveal microvascular abnormalities in diabetic retinopathy using optical coherence tomography angiography with projection artifact removal. *J Ophthalmol*. 2018;2018:3926745.
27. Yang JY, Wang Q, Yan YN, Zhou WJ, Jonas JB. Microvascular retinal changes in pre-clinical diabetic retinopathy as detected by optical coherence tomographic angiography. *Graefes Arch Clin Exp Ophthalmol*. 2020;258:1–8.
28. Inanc M, Tekin K, Kiziltoprak H, Ozalkak S, Doguizi S, Aycan Z. Changes in retinal microcirculation precede the clinical onset of diabetic retinopathy in children with type 1 diabetes mellitus. *Am J Ophthalmol*. 2019;207:37–44.
29. Chen Q, Ma Q, Wu C, et al. Macular vascular fractal dimension in the deep capillary layer as an early indicator of microvascular loss for retinopathy in type 2 diabetic patients. *Invest Ophthalmol Vis Sci*. 2017;58:3785–3794.
30. Frydkjaer-Olsen U, Soegaard Hansen R, Pedersen K, Peto T, Grauslund J. Retinal vascular fractals correlate with early neurodegeneration in patients with type 2 diabetes mellitus. *Invest Ophthalmol Vis Sci*. 2015;56:7438–7443.
31. Wang X, Han Y, Sun G, et al. Detection of the microvascular changes of diabetic retinopathy progression using optical coherence tomography angiography. *Transl Vis Sci Technol*. 2021;10:31.